J Math Chem (2009) 46:1188–1202
DOI 10.1007/s10910-008-9502-4

ORIGINAL PAPER

An analysis of nonlinear ion transport model including diffusion and migration

Alemdar Hasanov · Burhan Pektaş · Şafak Hasanoglu

Received: 5 November 2008 / Accepted: 24 November 2008 / Published online: 9 December 2008

Abstract The nonlocal identification problem related to nonlinear ion transport model including diffusion and migration is studied. Ion transport is assumed to be superposition of diffusion and migration under the influence of an electric field. Mathematical modeling of the experiment leads to an identification problem for a strongly nonlinear parabolic equation with nonlocal additional condition. Uniqueness of the nonlinear direct problem solution, and its continuity with respect to the total charge function is proved. An existence of a quasisolution of the identification problem is proved in the class of derived admissible coefficients. The nonlinear finite difference approximation of this problem, with an appropriate iteration algorithm, is derived. Numerical solutions of the identification problem are presented for various values of valences and diffusivities of oxidized and reduced oxidized species. The obtained results permits one to derive behaviour of the concentration and total charge depending on physical parameters.

Keywords Nonlinear ion transport · Nonlocal identification problem · Nonlinear parabolic problem · Current response · Iteration scheme

A. Hasanov · B. Pektaş (✉)
Department of Mathematics, Faculty Art and Sciences,
Kocaeli University, Umuttepe Kampusu, Izmit-Kocaeli 41380, Turkey
e-mail: burhanps@kocaeli.edu.tr; burhanps@gmail.com

Ş. Hasanoglu
Chemical-Engineering Division, Köseköy High School,
Kocaeli University, Umuttepe Kampusu, Izmit-Kocaeli, Turkey

1 Introduction

Mathematical modeling of kinetics and mass-transfer in electrochemical events and related electroanalytical experiments, generally consists of dealing with various physico-chemical parameters, as well as complicated mathematical problems, even in their simplest statement. These type of models are also complicated by the lack of a constitutive equations relating the electric field potential and the ion concentration (see, for instance [1–5] and references therein). Linear mathematical models of such problems in electrochemistry, in general, and in chronoamperometry, in particular, are usually based on the Nernst-Planck equation [1]. Analytical solutions of these simplest models permit one to understand experiment and to find out some relationships which can not be estimated experimentally. In chronoamperometry such a classical result has first been obtained experimentally by Cottrell [6]. In 1902 Cottrell derived a linear initial-boundary value problem (IBVP) and demonstrated that, if an extreme potential is suddenly applied to an electrode in contact with a solution containing a uniform concentration of an electroreactant, then the resulting current response $\mathcal{I}_C$, defined to be as Cottrellian, is proportional to $1/\sqrt{t}$. Subsequently this result has also been confirmed experimentally as well as theoretically. This relationship assumes that the ion transport is purely diffusive, planar and semi-infinite. Deviations from the ideal Cottrellian response provide information about complex chemical kinetics and kinetics of electron transfer. Further various modifications of the relationship $\mathcal{I}_C \sim 1/\sqrt{t}$ were investigated based on linear mathematical models. Thus, the transport response of electrodes under conditions of diffusion and migration was studied by Lange and Doblhofer [7]. They used the Nernst-Planck equation to derive a linear model for the transport of the electroactive species with zero initial condition. The problem then was solved by digital simulation techniques. For equal diffusion coefficients of all ions a linear model with an analytical formula and some numerical results have been obtained by Myland and Oldham [5]. Here the effect of migration factor to the limiting Cottrell currents was also studied. For the case of unequal diffusion coefficients this linear model was developed by Bieniasz [8]. Here the effects of the diffusivity ratio D_R/D_C, as well as of the electroactive and counter-ions on the limiting chronoamperometric currents were examined. Analytical formulas of the current response, and comparative analysis for linear models in chronoamperometry under conditions of diffusion and migration, have been given by Hasanov and Hasanoglu [9,10].

In the case of two-species migrating under the influence of the electric field, the *nonlinear mathematical model of mass and charge transport* in a controlled potential experiment have first been derived by Cohn, Pfabe and Redepenning [11]. In this model ion transport is assumed to be superposition of diffusion and migration. Although, due to lack of electrochemical information, this model is restricted to the two-species (oxidized and reduced) case, even in this simplest, from the point of view physico-chemical model, case the obtained mathematical problem is highly complicated, as we will see below. Specifically, in the case of two-species migrating under the influence of the electric field, the scaled mathematical model leads to the following problem [11]

$$\begin{cases} u_t = (g(u)u_x)_x + q'(t)h(u)_x, \quad (x,t) \in \Omega_\infty := (0,\infty) \times (0,\infty), \\ u(x,0) = 0, \quad x \in (0,\infty), \\ u(0,t) = 1, \quad t \in (0,\infty); \end{cases} \tag{1}$$

$$q(t) = \int_0^\infty u(x,t)dx, \quad t \geq 0, \tag{2}$$

with respect to the concentration $u(x,t)$ of the reduced species.

This is an identification problem for the nonlinear parabolic Eq. 1, with the additional nonlocal condition (2), and with respect to the unknown coefficient $q(t)$ (scaled total charge). The pair of functions $\langle u(x,t), q(t)\rangle$ will be defined as a solution of the identification problem (1)–(2).

The coefficients $g(u) > 0$ and $h(u)$ express an influence of the diffusion and migration in the ion transport, and have the forms [11]:

$$g(u) := \frac{z_0 + (z_r - z_0)u}{z_0 + (z_r\kappa - z_0)u}, \quad h(u) := \frac{\kappa u}{z_0 + (z_r\kappa - z_0)u}. \tag{3}$$

Here and below dimensionless parameter $\kappa := D_r/D_0$ represents the diffusivity ratio. The parameters z_r and z_0 denote the valences of the reduced and oxidized species.

The similarity solution $v(y)$, $y = x/\sqrt{t}$, of the nonlocal identification problem (1)–(2) satisfies the following nonlocal identification problem

$$\begin{cases} (g(v)v')' + \frac{1}{2}yv' + \frac{1}{2}ah(v)' = 0, \quad y \in R_+, \\ v(0) = 1, \\ v(\infty) = 0, \\ \\ \int_0^\infty v(y)dy = a > 0, \end{cases} \tag{4}$$

for the nonlinear ODE. An analysis of this model is given [11]. Based on the iteration scheme obtained in [11], various numerical algorithms for this one-dimensional identification problem have been proposed in [12–14].

Comparative computational analysis between linear model and the nonlinear model (1)–(2) has been studied in [15]. Due to mathematical as well as computational difficulties related to solving the nonlinear and nonlocal identification problem (1)–(2), as a first attempt, in [15] the nonlinear model (1)–(2) has been considered studied for the special case $\langle z_r, z_o\rangle = \langle -2, -1\rangle$. Computational results presented in [15] permit one to obtain upper and lower bounds for the scaled total charge, corresponding to the nonlinear model, via the appropriate upper and lower linear models.

The present work is aimed to study the nonlinear ion transport model (1)–(2), including diffusion and migration. Note that identification problems with nonlocal additional condition in integral form, arise also in convection-diffusion and settler models [16,17]. However in all these models parabolic equations are linear one.

In the next section some important physico-chemical and mathematical aspects of the nonlinear model (1)–(2), are derived. Reduction method for the identification problem is proposed in Sect. 3. The nonlinear finite-difference scheme for the reduced problem, and iteration algorithm are given in Sect. 4. In Sect. 5 computational

experiments related to behavior of the solution, depending on various values of valences and diffusivities of oxidized and reduced oxidized species, are presented. The final Sect. 6 contains some conclusions.

2 Preliminary analysis of the nonlinear ion transport model

Although the mathematical model of the nonlinear ion transport problem is given in [11], for completeness, we briefly discuss here some distinguished features of this scaled model. The general background of the physico-chemical aspects of the problem can be found in [1,4].

Let $x \geq 0$ and $t \geq 0$ be the scaled space and time variables. To describe a standard experiment, we assume that there is an electrode at $x = 0$, and a polymeric medium containing mobile ions and electroactive species extending from the electrode to $x = \infty$. It is assumed that the electroactive species are in oxidized form before the time $t = 0$. At $t = 0$ a potential E is introduced at the electrode. This causes a fraction of the oxidized species at the surface of the electrode to be reduced. We denote by $u = u(x, t)$ and $D_r > 0$ the scaled concentration and diffusion of the *reduced species*. As oxidized species are reduced at the surface of the electrode, its concentration decreases, and the concentration $u = u(x, t)$ of the reduced species at the electrode increases. As a result there arise two diffusion processes: oxidized species diffuse in toward $x = 0$, and the reduced species diffuse out into the medium. Therefore ion transport here can be regarded as a superposition of *diffusion*, which is a random motion of small particles immersed in the medium, and *migration*, which is a motion under the influence of an electric field. Exchange of electrons between the surface of the electrode and electroactive species in the time $t > 0$ gives rise to the *current response* $\mathcal{I} = \mathcal{I}(t)$, which is related to the concentration of reduced species by the balance equation [1]

$$\frac{u_0}{z_r} \int_0^\infty u(x, t)dx = \frac{1}{n\mathcal{F}S_e} \int_0^t \mathcal{I}(\tau)d\tau. \tag{5}$$

Here n is the number of electrons gained by an ion upon reduction, $\mathcal{F}$ is Faraday's constant, S_e is the surface area of the electrode, and u_0 is the concentration at $x = 0$ of the reduced species at the electrode. The total charge carried by the reduced species is defined to be

$$Q(t) = \int_0^t \mathcal{I}(\tau)d\tau.$$

These two definitions permit one to define the total charge $Q(t)$ and the current response $\mathcal{I}(t)$ via the concentration $u = u(x, t)$ of the reduced species:

$$Q(t) = \frac{n\mathcal{F}S_e u_0}{z_r} \int_0^\infty u(x, t)dx, \quad \mathcal{I}(t) = \frac{n\mathcal{F}S_e u_0}{z_r} \int_0^\infty u_t(x, t)dx. \tag{6}$$

Hence the scaled total charge $q(t)$ defined by (2) is

$$q(t) = \frac{z_r}{n\mathcal{F}S_e u_0} Q(t). \tag{7}$$

As was established experimentally in [2], for extremely high voltage perturbation, the concentration of oxidized species at the electrode drops immediately to zero, and, at the same time, the concentration $u(x,t)$ of the reduced species at the electrode ($x = 0$) is made to jump from zero to u_0/z_r. The process of perturbing the voltage in this manner and studying the resulting current response $\mathcal{I}_C(t)$ as a function of time is known as *chronoamperometry* [1]. In the case of *purely diffusive* flux of electroactive species, a relationship between the time $t > 0$ and the current response $\mathcal{I}_C$ has first been experimentally obtained in 1902 by Cottrell. He was found that the current response is proportional to $1/\sqrt{t}$:

$$\mathcal{I}_C \sim 1/\sqrt{t}.$$

This relationship is defined to be Cottrellian. The theoretical analysis of this relationship has been given by Cohn in [11], based on the purely diffusive mathematical model

$$\begin{cases} u_t = Du_{xx}, & (x,t) \in R_+ \times R_+, \quad R_+ = (0,+\infty), \\ u(x,0) = 0, & x \in R_+, \\ u(0,t) = u_0/z_r, & t \in R_+. \end{cases}$$

The analytical formula obtained here for Cottrellian is as follows:

$$\mathcal{I}_C(t) = \frac{n\mathcal{F}S_e u_0}{z_r}\sqrt{\frac{D}{\pi t}}. \tag{8}$$

Taking into account (6)–(7) we may conclude that the scaled total charge $q(t)$, defined by (2), is proportional to $\sqrt{t}$. However this result is valid for a purely diffusive mathematical model, and presence of any migration term in the above parabolic equation leads to essential deviations from the Cottrellian, as the results presented in [10] show. Moreover, influence of the valences z_r and z_0 of the reduced and oxidized species, as well as an influence of the diffusivity ratio $\kappa > 0$, are not taken into account in this model.

We will consider the mathematical model (1)–(2) under the following assumptions:

(A1) $u(\infty,t) = u_x(\infty,t) = 0, \forall t > 0$;
(A2) $z_r D_r = z_o D_o$.

Assumption (A1) is based on experimental and theoretical results (see, [11] and references therein), obtained for the nonlinear model (1)–(2). Namely, these results show that for a fixed time $t \in (0,\infty)$, the concentration function $u(x,t)$ and its partial derivative $u_x(x,t)$ decreases rapidly to zero, as $x \to \infty$, for all $t > 0$. In this study, we will only assume $u(L,t) = 0$, where $L > 0$ is a large enough number, taking into

Table 1 The admissible values of valences and corresponding values of diffusivity ratio

$\langle z_r, z_0\rangle$	$\langle -4, -3\rangle$	$\langle -3, -2\rangle$	$\langle -2, -1\rangle$	$\langle 1, 2\rangle$	$\langle 2, 3\rangle$
$\kappa = D_r/D_0$	3/4	2/3	1/2	2.0	3/2

account the property $u(x,t) \to 0$, as $x \to \infty$, $\forall t > 0$ of the concentration function $u(x,t)$.

Although the assumption (A2) makes some restriction for values of diffusivities D_r and D_0, it still permits one to analyze the nonlinear model (1)–(2) for real class of materials. Specifically, under the assumption $z_r D_r = z_0 D_0$, the diffusivity ratio $\kappa = D_r/D_0$ can be defined via the valences as follows: $\kappa = z_0/z_r$. According the admissible values of the valences, given in Table 1, the parameter κ assumes appropriate values in the interval $[0.5,\ 2]$. In terms of the considered physical model these values are large enough for theoretical analysis of the considered experiment, since include the both cases $\kappa < 1$ (diffusivity of oxidized species dominates) and $\kappa > 1$ (diffusivity of the reduced species dominates). Note that, the similar values of the diffusivity ratio κ are used in experimental studies (see, [2,5]).

Under the assumption (A2) the functions $g(u)$ and $h(u)$, defined by (3), have the following forms:

$$g(u) := 1 + \left(\frac{z_r}{z_0} - 1\right) u, \quad h(u) := \frac{1}{z_r} u, \tag{9}$$

and the nonlinear term $h(u)_x$ in the parabolic Eq. 1 becomes $h(u)_x := u_x/z_r$. Thus, with the above assumptions (A1)-(A2) the mathematical model (1)–(2) can be replaced by the following identification problem in the bounded domain $\Omega_T := (0, L) \times (0, T]$:

$$\begin{cases} u_t = (g(u)u_x)_x + \frac{1}{z_r} q'(t) u_x, \quad (x,t) \in \Omega_T, \\ u(x,0) = 0, \quad x \in (0, L), \\ u(0,t) = 1, \ \ u(L,t) = 0, \quad t \in (0, T]; \end{cases} \tag{10}$$

$$q(t) = \int_0^L u(x,t)dx, \ \ t \in [0, T]. \tag{11}$$

Since the considered mathematical model is a scaled one, the values of concentration function $u(x,t)$ are in $[0, 1]$, i.e. it satisfies the following condition:

$$0 \le u(x,t) \le 1, \ \ \forall (x,t) \in \Omega_T. \tag{12}$$

Problem (10)–(11) will be defined as the *nonlocal identification problem* in the bounded domain $\Omega_T := (0, L) \times (0, T]$. Accordingly, for a given coefficient $q(t)$, as well as for given parameters κ, z_r, z_0, and functions $g(u)$ and $h(u)$, defined by (9), the nonlinear initial-boundary value problem (10) will be defined as the *direct problem*.

3 Reduction method for the identification problem (10)–(11)

Let us consider first the nonlinear direct problem (10). To define an appropriate class of weak solutions of this problem we assume that $q(t) \in \mathcal{Q}$ is a given function from some class of admissible coefficients $\mathcal{Q}$, which will be defined below. Multiply the both sides of the nonlinear parabolic equation to the function $u(x,t)$, and then integrate on $\Omega_t := (0,L)\times(0,t]$, $t \in (0,T]$. Applying integration by parts and then using elementary transformations we obtain:

$$\begin{aligned}\frac{1}{2}\int_0^L\int_0^t u_t^2(x,t)d\tau dx + \int_0^t\int_0^L g(u)u_x^2(x,\tau)dxd\tau \\ = \int_0^t [g(u(L,\tau))u_x(L,\tau)u(L,\tau) - g(u(0,\tau))u_x(0,\tau)u(0,\tau)]d\tau \\ + \frac{1}{z_r}\int_0^t q'(\tau)\int_0^L u(x,\tau)u_x(x,\tau)dxd\tau, \quad t\in(0,T].\end{aligned}$$

Taking into account the initial and boundary conditions $u(x,0) = 0$, $u(0,t) = 1$, $u(L,t) = 0$, $t \in (0,T]$, and the condition $u_x(L,t) = 0$, after integrating we get:

$$\begin{aligned}\frac{1}{2}\int_0^L u^2(x,t)dx + \int_0^t\int_0^L g(u)u_x^2(x,\tau)dxd\tau \\ = -\frac{1}{\kappa}\int_0^t u_x(0,\tau)d\tau - \frac{1}{2z_r}q(t), \quad t\in(0,T].\end{aligned} \tag{13}$$

This energy identity provides further insight into the weak solution class for the direct problem. Specifically, the left hand side is well-defined for all functions $u \in \mathring{V}^{1,0}(\Omega_T)\cap C^1(\Omega_T)$, $\mathring{V}^{1,0}(\Omega_T) \subset V^{1,0}(\Omega_T)$, where $V^{1,0}(\Omega_T)$ is the Banach space of functions with the norm ([18])

$$\|u\|_{V^{1,0}(\Omega_T)} = \max_{t\in[0,T]}\|u\|_{H^0(0,L)} + \|u_x\|_{H^0(\Omega_T)}, \tag{14}$$

and $\mathring{V}^{1,0}(\Omega_T) := \{u \in V^{1,0}(\Omega_T) : u(L,t) = 0\}$. Here and below $\|\cdot\|_{H^p(0,L)}$ and $\|\cdot\|_{H^p(\Omega_T)}$ are norms of the Sobolev spaces $H^p[0,L]$ and $H^p(\Omega_T)$, respectively. Note that due to the homogeneous Dirichlet boundary condition $u(L,t) = 0$, the norms $\|u_x\|_{H^0(\Omega_T)}$ and $\|u\|_{H^1(\Omega_T)}$ are equivalent.

Thus, by the above conclusions, we will look for a solution of the direct problem (10) in the Banach space $\mathring{V}^{1,0}(\Omega_T)$, assuming additionally $u \in C^1(\Omega_T)$. Evidently, all integral in (13) are continuous in $t \in [0,T]$. Therefore, the natural requirement for the coefficient $q(t)$ is its continuity: $q(t) \in C[0,T]$.

The left hand side of (13) is defined to be the energy integral.

Let us integrate now the both sides of the parabolic Eq. 10 on $\Omega_t := (0,L)\times(0,t]$, $t \in (0,T]$:

$$\int_0^L\int_0^t u_\tau dxd\tau = \int_0^t\int_0^L (g(u)u_x)_x dxd\tau + \frac{1}{z_r}\int_0^t q'(\tau)\int_0^L u_x dxd\tau, \quad t\in(0,T].$$

Calculating the integrals we obtain:

$$\int_0^L u(x,t)dx = \int_0^t [g(u(L,t))u_x(L,t) - g(u(0,t))u_x(0,t)]d\tau + \frac{1}{z_r}\int_0^t q'(\tau)[u(L,t) - u(0,t)]d\tau, \quad t \in (0,T].$$

Using here the conditions $u(L,t) = u_x(L,t) = 0$, $u_x(0,t) = 1$, also, $g(u(0,t)) = g(1) = 1/\kappa$, we get

$$\int_0^L u(x,t)dx = -\frac{1}{\kappa}\int_0^t u_x(0,\tau)d\tau - \frac{1}{z_r}\int_0^t q'(\tau)d\tau, \quad t \in (0,T].$$

Therefore

$$\int_0^L u(x,t)dx = -\frac{1}{\kappa}\int_0^t u_x(0,\tau)d\tau - \frac{1}{z_r}q(t), \quad t \in (0,T], \tag{15}$$

since $q(0) = 0$.

Let us assume now that $q(t) \in \mathcal{Q}_{\text{ad}}$ is the solution of the identification problem (10)–(11). Then using the nonlocal additional condition (11) on the left hand side of (23) we find:

$$q(t) = -\frac{z_r}{(1+z_r)\kappa}\int_0^t u_x(0,\tau)d\tau, \quad t \in [0,T]. \tag{16}$$

Differentiating formally the both sides and substituting in the parabolic Eq. 10 we obtain the following reduced identification problem:

$$\begin{cases} u_t = (g(u)u_x)_x - \frac{1}{(1+z_r)\kappa}u_x(0,t)u_x, & (x,t) \in \Omega_T, \\ u(x,0) = 0, \quad x \in (0,L), \\ u(0,t) = 1, \ \ u(L,t) = 0, \quad t \in (0,T]; \end{cases} \tag{17}$$

Proposition 3.1 *The pair $\langle u(x,t),\ q(t)\rangle$, $u(x,t) \in \mathring{V}^{1,0}(\Omega_T)$, $q(t) \in \mathcal{Q}_{ad}$ is the solution of the identification problem (10)–(11), if only if, the function $u(x,t) \in \mathring{V}^{1,0}(\Omega_T)$ is the solution of the nonlinear initial-boundary value problem (17).*

We use now formula (16) on the right hand side of identity (13). We have:

$$\frac{1}{2}\int_0^L u^2(x,t)dx + \int_0^t\int_0^L g(u)u_x^2(x,\tau)dxd\tau = -\frac{1+2z_r}{2\kappa(1+z_r)}\int_0^t u_x(0,\tau)d\tau, \quad t \in (0,T]. \tag{18}$$

This integral identity is defined to be the energy identity for the reduced identification problem (17).

Formula (16) also permits one to express the scaled total charge $q(t)$ via the total value of the left flux at $x = 0$, during the time $t \in (0, T]$. Indeed, by the physical definition of the flux at $x = 0$, $\mathcal{J}_0(t) = -(g(u)u_x(x,t))_{x=0}$. Since $g(u(0,t)) = 1/\kappa$, we have $\mathcal{J}_0(t) = -u_x(0,t)/\kappa$. Taking into account this in (16) we obtain:

$$q(t) = \frac{z_r}{(1+z_r)} \int_0^t \mathcal{J}_0(\tau) d\tau, \quad t \in [0, T]. \tag{19}$$

Furthermore, formula (19) with the energy identity (18), and with the definition $\mathcal{J}_0(t) = -u_x(0,t)/\kappa$ allows to define the sign of the flux $\mathcal{J}_0(t)$, at $x = 0$. Indeed, since $(1 + 2z_r)/(2\kappa(1 + z_r)) > 0$ for all admissible values of valences, the identity (18) implies that the flux $\mathcal{J}_0(t)$ at $x = 0$ is positive:

$$\mathcal{J}_0(t) = -\frac{1}{\kappa} u_x(0,t) > 0, \quad t \in (0, T]. \tag{20}$$

This result agrees with the physical meaning of the flux.

Thus, the nonlinear identification problem (10)–(11) is reduced to the nonlinear initial-boundary value problem (17), which does not contain the function $q(t)$. The main distinguished feature of this approach is that the problem of solving the coupled problem (10)–(11) is separated into the two subproblems: solving the nonlinear parabolic problem (17), and then finding the function $q(t)$ by the integration formula (11).

4 The numerical algorithm and test examples

We derive here an iteration algorithm for the reduced problem (17), using an implicit finite difference scheme for the linearized reduced problem:

$$\begin{cases} u_t^{(n)} = (g(u^{(n-1)})u_x^{(n)})_x - \frac{1}{(1+z_r)\kappa}\, u_x^{(n-1)}(0,t) u_x^{(n)}, & (x,t) \in \Omega_T, \\ u^{(n)}(x,0) = 0, \quad x \in (0, L), \\ u^{(n)}(0,t) = 1, \;\; u^{(n)}(L,t) = 0, \quad t \in (0, T]. \end{cases} \tag{21}$$

Denote by $v(x,t) = u^{(n)}(x,t)$, $\tilde{g}(x,t) = g(u^{(n-1)}(x,t))$, $\nu(t) = u_x^{(n-1)}(0,t)/((1 + z_r)\kappa)$. Then the linearized reduced problem (21) can be rewritten in the form of the initial-boundary value problem for the linear advection-diffusion equation:

$$\begin{cases} v_t = (\tilde{g}(x,t))v_x)_x - \nu(t)v_x, & (x,t) \in \Omega_T, \\ v(x,0) = 0, \quad x \in (0, L), \\ v(0,t) = 1, \;\; v(L,t) = 0, \quad t \in (0, T]. \end{cases} \tag{22}$$

To solve the linearized reduced problem (22) we define the uniform space and time grids

$$\overline{w}_h = \{x_i \in (0,l] : x_i = ih_x;\ i = \overline{0, N_x},\ h_x = l/N_x\},$$
$$\overline{w}_\tau = \{t_j \in (0,T] : t_j = jh_t;\ j = \overline{0, N_t},\ h_t = T/N_t\},$$

and use the standard finite difference approximations

$$u_{x,ij} := \frac{u_{i+1,j} - u_{i,j}}{h_x},\ u_{t,ij} := \frac{u_{i,j+1} - u_{i,j}}{h_t},\ u_{i,j} := u(x_i, t_j),\ i = \overline{1, N},\ j = \overline{1, M}$$

of the partial derivatives $\partial u/\partial x$, $\partial u/\partial t$. Here the constants $h_x > 0$ and $h_t > 0$ are the grid parameters.

For the numerical solution of the linear parabolic problem (22) we use the following implicit monotone difference scheme [19]

$$\begin{cases} \frac{v_{i,j+1}-v_{i,j}}{h_t} - \frac{1}{h_x}\left[\tilde{g}(x_{i+1/2}, t_j)\frac{v_{i+1,j+1}-v_{i,j+1}}{h_x} - g(x_{i-1/2}, h_j)\frac{v_{i,j+1}-v_{i-1,j+1}}{h_x}\right] \\ +\nu(t_j)\frac{v_{i+1,j+1}-v_{i-1,j+1}}{2h_x} = 0,\quad i = \overline{1, N_x - 1},\quad j = \overline{1, N_t - 1}; \\ v_{i,0} = 0,\quad i = \overline{0, N_x}, \\ v_{0,j} = 1,\ v_{N_x,j} = 0,\quad j = \overline{1, N_t}, \end{cases} \tag{23}$$

which has the accuracy $O(h_x^2 + h_t)$ on the uniform grid $w_{ht} = w_h \times w_t$.

4.1 Numerical test for the discrete problem (23)

The function

$$u(x,t) = exp(-tx^2),\quad x \in [0,4],\quad t \in [0,1]$$

is the analytical solution of the linear parabolic problem

$$\begin{cases} v_t = (\tilde{g}(x,t))v_x)_x - \nu(t)v_x + f(x,t), \quad (x,t) \in \Omega_T, \\ v(x,0) = \varphi(x), \quad x \in (0,L), \\ v(0,t) = \mu_1(t),\quad v(l,t) = \mu_2(t), \quad t \in (0,T], \end{cases}$$

with the given coefficients

$$\tilde{g}(x,t) = 1 + x^2, \quad \nu(t) = \sqrt{t},$$

and the source term

Table 2 Numerical results for the linear problem on different grids

h_x (N_x)	h_t (N_t)	$R = h_t/h_x^2$	$\varepsilon_v := \|v - v_h\|_\infty$	η_t
0.1 (41)	0.05 (21)	5.0	5.52×10^{-2}	–
0.05 (81)	0.05 (21)	20.0	5.52×10^{-2}	–
0.05 (81)	0.025 (41)	10.0	2.96×10^{-2}	0.8991
0.05 (81)	0.125 (81)	5.0	1.54×10^{-2}	0.9427
0.05 (81)	0.0063 (161)	2.5	7.8×10^{-3}	0.9814

$$f(x,t) = \{-x^2 + 2t[3x^2 - 2x^2t(x^2+1) + 1] + 2xt\sqrt{t}\}\exp(-tx^2),$$

and appropriately chosen functions $\varphi(x)$, $\mu_1(t)$, $\mu_2(t)$, obtained from the above analytical solution.

Table 2 shows the absolute sup-norm errors obtained on different grid parameters N_x, N_t. The last column of the table shows the approximation errors defined as

$$\eta_t = \frac{\log(\varepsilon_t^{(1)}/\varepsilon_t^{(2)})}{\log(N_t^{(2)}/N_t^{(1)})}.$$

These errors correspond to the time grids given on the last three lines of the Table 2. The smallest absolute error $\varepsilon_v = 7.8 \times 10^{-3}$ is obtained on the grid of size $N_x \times N_t = 81 \times 161$, with $R = 2.5$, as the last line of the table shows. This grid will be used in subsequent computational experiments.

4.2 Numerical test for the nonlinear problem (17)

In this example we apply the linearization scheme (21) to the nonlinear problem

$$\begin{cases} u_t = (g(u)u_x)_x - v(t)u_x + f(x,t), & (x,t) \in \Omega_T, \\ u(x,0) = \varphi(x), & x \in (0,L), \\ u(0,t) = \mu_1(t), \quad u(L,t) = \mu_2(t), & t \in (0,T], \end{cases} \tag{24}$$

with the coefficient $g(u)$, given by (9), and with the parameter $\kappa = 0.5$. The coefficient $v(t)$ is chosen as $v(t) = \sqrt{t}$, taking into account the relationship $q(t) \sim \sqrt{t}$ for the classical Cottrellian. The analytical solution

$$u(x,t) = exp(-tx^2), \quad x \in [0,4], \quad t \in [0,1]$$

of problem (24) corresponds to the source term

$$f(x,t) = \{-x^2 - 4x^2t^2(\kappa - 1)\exp(-tx^2) - g(u)(4x^2t^2 - 2t - 2xtv(t))\} \times \exp(-tx^2),$$

and to appropriately chosen functions $\varphi(x)$, $\mu_1(t)$, $\mu_2(t)$.

Table 3 Numerical results for the nonlinear problem on different grids

h_x (N_x)	h_t (N_t)	$R = h_t/h_x^2$	$\varepsilon_u := \|u - u_h\|_\infty$	Iteration number	η_t
0.05 (81)	0.025 (41)	10.0	9.08×10^{-2}	4	0.9014
0.05 (81)	0.125 (81)	5.0	4.70×10^{-2}	4	0.9500
0.05 (81)	0.0063 (161)	2.5	2.39×10^{-2}	4	0.9757

The nonlinear problem (24) was solved by applying the iteration scheme (21). The condition $\varepsilon_{it} := \|u_h^{(n+1)} - u_h^{(n)}\|_\infty$, with $\varepsilon_{it} = 10^{-3}$ was used as a stopping criteria for the iteration process. Numerical results obtained on different grids are shown in Table 3.

The absolute sup-norm errors obtained for different grid parameters N_x, N_t are given in the fourth column of the table. As the fifth column of the table shows, the number of iterations does not increase, by increasing the grid sizes. Further, the approximation error η_t tends to 1 by increasing the grid size. This result agrees with the order of approximation $O(h_t)$ of the difference scheme (23), with respect to time mesh parameter h_t.

All these results show that the accuracy of the above discrete model is high enough.

5 Further computational experiments and discussions

In this section we discuss results of computational experiments related to the reduced identification problem (17). Based on these results we will analyze the behavior of the concentration function $u(x, t)$ with respect to the time $t > 0$ and space $x > 0$ variables. Then we study an influence of valences z_0, z_r of the oxidized and reduced species, and also the diffusivity ratio $\kappa = D_r/D_0$, to the behavior of the scaled total charge $q(t)$.

The numerical solutions of the reduced identification problem (17), obtained by the above iteration algorithm, are plotted in Fig. 1. These solutions correspond to the admissible values $\langle z_0, z_r\rangle = \langle -2, -3\rangle$; $\langle -3, -4\rangle$; $\langle 2, 1\rangle$; $\langle 3, 2\rangle$ of valences, and the diffusivity ratio $\kappa = 0.5$. As show all figures, for fixed time $t > 0$ the solution $u_h^{(n)}(x, t)$ decreases rapidly and monotonically on the space interval [0, 1]. Further, in all cases the solutions are smooth functions. These results agree with the theoretical results proposed in [11], as well as with the experimental results described in [1,2]. These figures also show that the behavior of the concentration function $u(x, t)$ with respect to the time variable $t > 0$, and with respect to the space variable $x \in [0, L]$, are different. Specifically, for fixed space variable $x > 0$, the solution $u_h^{(n)}(x, t)$ increases slowly and monotonically from 0 to 1 in the time interval [0, 1]. At the same time, for fixed time variable $t > 0$, this solution decreases rapidly and monotonically in the space interval [0, 1].

The second part of computational experiments is related to the behavior of the scaled total charge $q(t)$ depending on the values of valences given in Table 1. Figure 2 shows the profiles of the total charge $q_h(t)$. These functions are obtained from the

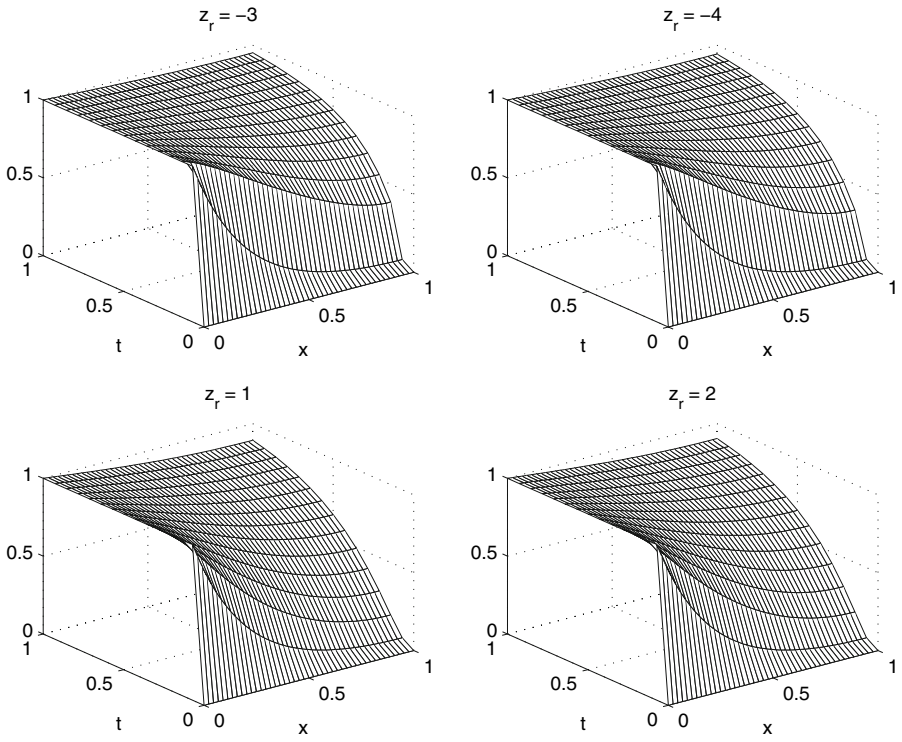

Fig. 1 Numerical solutions $u_h^{(n)}$ of the reduced identification problem (17), corresponding to different values of valences of the oxidized and reduced species

corresponding numerical solutions $u_h(x,t)$ of the reduced problem (17), with subsequent calculation of the integral (11), by the numerical integration trapezoidal formula. The profiles of the total charge $q_h(t)$ plotted in Fig. 2 correspond to the four admissible values of the valences, given in Table 1. The solid line in the middle is the function $q_C(t) = \sqrt{t}$, which corresponds to the classical Cottrellian. The lower two graphs correspond to the positive values of valences z_0 and z_r, while the upper three graphs correspond to the negative ones. For all negative z_0 and z_r, the migrational and diffusional contributions to the flux of the reduced species act in the same direction. Hence, the resulting contributions to the flux of the reduced species extend further from the electrode than the purely diffusional profile. This conclusion is consistent with the values of the scaled total charge $q(t)$, plotted in Fig. 2 (upper from the classical Cottrellian), and corresponding to the negative values of valences. Further, for positive values of valences, the migrational and diffusional contributions to the flux of the reduces species act in the opposite directions. Consequently, in this case mass transfer of the reduced species away from the electrode is less facile that in purely diffusive case. The corresponding values of the scaled total charge $q(t)$, plotted in Fig. 2 (under the classical Cottrellian), is also consistent with this conclusion.

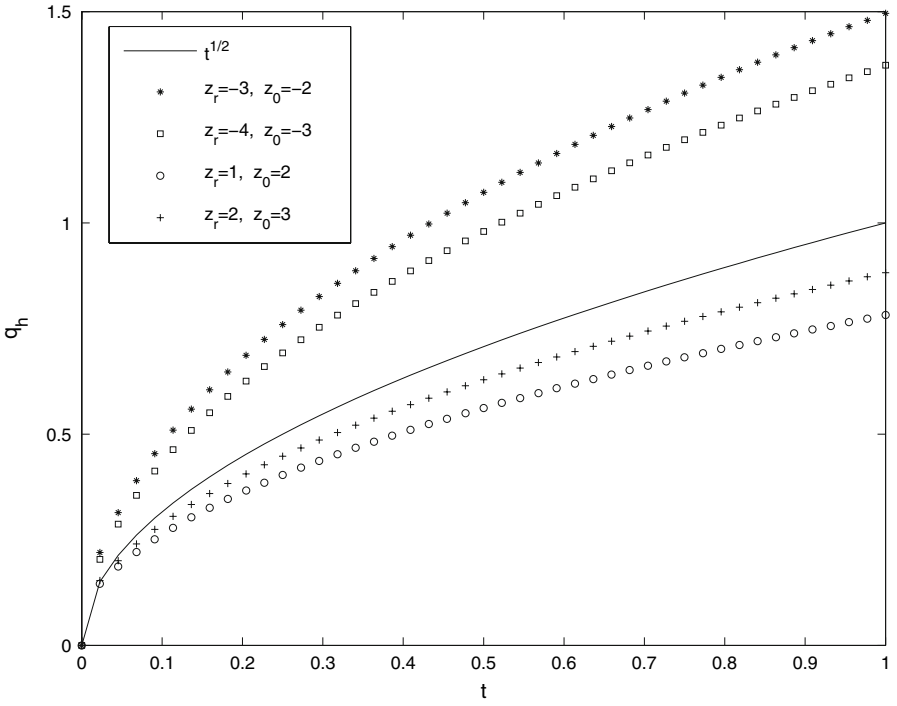

Fig. 2 The identified function $q_h(t)$ corresponding to the different values of the valences

The above computational results permit also to analyze an influence of the diffusivities D_r and D_0 of the oxidized and reduced species to the behavior of the scaled total charge $q(t)$. Due to the relationship $\kappa = z_0/z_r = D_r/D_0$, the values of valences of the oxidized and reduced species, given on the first line of Table 1, correspond to the values of the diffusivity ratio $\kappa > 0$, given, on the second line of Table 1. Enumerating these values in the increasing order, as

$$\kappa_1 = 1/2 < \kappa_2 = 2/3 < \kappa_3 = 3/4 > \kappa_4 = 3/2 < \kappa_5 = 2,$$

we can see from Fig. 2 that the mapping $\kappa \mapsto q[\kappa]$ is an antitone one:

$$\kappa_i < \kappa_{i+1} \quad \Rightarrow \quad q[\kappa_i] > q[\kappa_{i+1}].$$

The reason of this phenomenon is that, for a given diffusivity D_r of the reduced species, the diffusivity $D_0^{(i)}$ of the oxidized species is defined via the diffusivity ratio $\kappa_i > 0$, is as follows: $D_0^{(i)} = D_r/\kappa_i > 0$. Hence the above increasing values $\kappa_i < \kappa_{i+1}$ of the diffusivity ratio correspond to the decreasing values $D_0^{(i)} > D_0^{(i+1)}$ of the oxidized species. As it was noted in the physical model, the concentration $u = u(x,t)$ of the reduced species at the electrode increases, as oxidized species are reduced. Hence $u[D_0^{(i)}] > u[D_0^{(i+1)}]$, which implies $q[\kappa_i] > q[\kappa_{i+1}]$.

6 Conclusions

In this paper, we analyzed the mathematical model of the nonlinear ion transport problem, which includes diffusion and migration. We derive a new method of solution, reducing the identification problem to the initial-boundary problem for strongly nonlinear parabolic equation, by eliminating the nonlocal additional condition. Based on this method we propose a numerical iteration algorithm for solving the identification problem. The theoretical results have been validated using real physical parameters. The presented computational results are consistent with their physical meaning and experimental results for real systems.

Acknowledgements The research has been supported by the Scientific and Technological Research Council of Turkey (TUBITAK) through the project Nr 108T332.

References

1. A.J. Bard, L.R. Faulkner, in *Electrochemical Methods* (Wiley, New York, 1980)
2. R.P. Buck, M.B. Madaras, R. Mäckel, Diffusion-migration capacitance in homogeneous membranes, modified electrodes and thin-layer cells. J. Electroanal. Chem. **366**, 55–68 (1994)
3. W. Kucza, M. Danielewski, A. Lewenstam, Electrochem. Commun. **8**, 416 (2002)
4. L. Liberti, F.G. Helffrich, in *Mass Transfer and the Kinetics of Ion Exchange* (NATO ASI Series) (Martinus Mijhoff, Boston, 1987)
5. J.C. Myland, K.B. Oldham, Electrochem. Commun. **1**, 467 (1999)
6. F.G. Cottrell, Z. Phys. Chem. **42**, 385 (1903)
7. R. Lange, K. Doblhofer, J. Electroanal. Chem. **237**, 13 (1987)
8. L.K. Bieniasz, Electrochem. Commun. **4**, 917 (2002)
9. A. Hasanov, Şafak Hasanoglu, Math. Chem. **42**, 741 (2007)
10. A. Hasanov, Şafak Hasanoglu, Math. Chem. **44**, 133 (2008)
11. S. Cohn, K. Pfabe, J. Redepenning, Math. Mod. Meth. Appl. Sci. **9**, 455 (1999)
12. A. Hasanov, Math. Meth. Appl. Sci. **21**, 1195 (1998)
13. A. Hasanov, J.L. Mueller, S. Cohn, J. Redepenning, Comput. Math. Appl. **39**, 225, (2000)
14. K. Pfabe, T.S. Shores, Appl. Numer. Math. **32**, 175 (2000)
15. A. Hasanov, Şafak Hasanoglu, Math. Chem. **44**, 731 (2008)
16. J.P. Chancelier, M. Cohen de Lara, F. Pacard, Math. Mod. Meth. Appl. Sci. **5**, 267 (1995)
17. S. Lenhart, Math. Mod. Meth. Appl. Sci. **5**, 225 (1995)
18. O. Ladyzhenskaya, V. Solonnikov, N. Uraltseva, in *Linear and Quasilinear Equations of Parabolic Type* (AMC, Providence, 1968)
19. A.A. Samarskii, in *The Theory of Difference Schemes* (Marcel Dekker, New York, 2001)